

On the non-linear scale of cosmological perturbation theory

Diego Blas^a, Mathias Garny^b, Thomas Konstandin^b

^a *CERN, Theory Division, 1211 Geneva, Switzerland*

^b *DESY, Notkestr. 85, 22607 Hamburg, Germany*

Abstract

We discuss the convergence of cosmological perturbation theory. We prove that the polynomial enhancement of the non-linear corrections expected from the effects of soft modes is absent in equal-time correlators like the power or bispectrum. We first show this at leading order by resumming the most important corrections of soft modes to an arbitrary skeleton of hard fluctuations. We derive the same result in the eikonal approximation, which also allows us to show the absence of enhancement at any order. We complement the proof by an explicit calculation of the power spectrum at two-loop order, and by further numerical checks at higher orders. Using these insights, we argue that the modification of the power spectrum from soft modes corresponds at most to logarithmic corrections at any order in perturbation theory. Finally, we discuss the asymptotic behavior in the large and small momentum regimes and identify the expansion parameter pertinent to non-linear corrections.

1 Introduction

The theory of cosmological perturbations is the standard tool to understand the emergence of the large scale structure of the Universe [1, 2]. This approach is based on the assumption that small perturbations around an otherwise homogeneous and isotropic Universe grow with time due to their gravitational interaction. This growth is particularly efficient for scales inside the Hubble horizon and in the matter-dominated epoch [1]. The tiny amplitude of the primordial perturbations allows for a perturbative treatment of this non-linear problem, but the aforementioned growth eventually invalidates this approach. The scale at which this happens has been traditionally identified with moments of the linear power spectrum. A particularly interesting scale is created by the enhancement of non-linearity coming from the coupling of modes of small momenta (*soft*) to the modes of the scale of interest (*hard*),

$$k_{NL}^{-2} \sim \int dq P^L(q, \eta), \quad (1)$$

where $P^L(q, \eta)$ is the linear power spectrum at time η (we will be more precise about this point below). To study physics beyond this scale, it seems unavoidable to resort to non-perturbative schemes. Particularly well-suited to deal with this effect is the scheme known as renormalized cosmological perturbation theory (RPT) [3]. This systematic approach to cosmological perturbation theory is based on the introduction of the non-linear propagator, for which the non-linear effects associated to the scale (1) were derived in [4]. These result in an exponential suppression controlled by k_{NL} that was also conjectured to be the leading effect in the matter power spectrum.

The seminal work [3] was followed by many other resummation schemes put forward to cope with non-linear effects in an analytical way (i.e. without resorting to large N -body simulations) [5, 6, 7, 8, 9, 10]. The hope is that after resummation of a subset of diagrams the resulting expansion is under better control. For schemes related to the effects of the scale (1) in the power spectrum this expectation is at odds with two results. First, it is known since a long time that the leading contributions to the power spectrum from soft modes at arbitrary loop order cancel [11, 12]. In the above mentioned resummation schemes this cancellation is normally not explicit. Second, one can try to systematically understand the effects of soft modes on hard modes by using the *eikonal* approximation [13]. In this case, it was shown that the mentioned suppression for the propagator is present while the power

spectrum is unchanged [14]. A first aim of this work is to reconcile both approaches and understand how the eikonal result can be recovered from the diagrammatic technique of resummation of soft modes.

The cancellation of the effects from soft modes suggests that the convergence properties of standard perturbation theory (SPT) are not ameliorated by resumming the soft modes. It also suggests that the effects in the power spectrum associated to k_{NL} are spurious, which immediately rises the question of what is the real parameter governing the non-linear corrections for this observable, also in SPT. It is simpler to answer this point after implementing the eikonal approximation in a controllable way. We will do this in the second part of the paper. The scale (or parameter) controlling the non-linear dynamics in this case, and not (1), should be the one tamed by any resummation scheme with a better validity than the standard case for the non-linear dynamics.

Our work is organized as follows: Section 2 clarifies our notation and reviews standard perturbation theory (SPT). Section 3 discusses the two main resummation schemes we are concerned with, namely renormalized perturbation theory (RPT) and the eikonal approximation. In section 4 we generalize the resummation of RPT to a larger class of soft corrections that are relevant to the power spectrum and other equal-time correlators. This motivates the discussion of next-to-leading order corrections in the eikonal approximation presented in section 5. The main result is that no enhancement from soft vertices should be present in equal-time correlators. We further support these claims by explicit analytic and numerical results presented in section 6. We conclude in section 7. Some technical details are relegated to the Appendices.

2 Standard cosmological perturbation theory

In this section we set up the system of equations relevant for our discussion. As stated in the introduction, we are interested in understanding some features about the behavior of cosmological perturbations when their amplitude grows to the point that non-linear corrections are important. For this problem it is enough to consider sub-horizon perturbations in a matter-dominated

era. We will also assume¹ that the matter in the Universe is a perfect fluid described by a density field $\rho(x, \tau) = \rho(t)(1 + \delta(x, \tau))$ and a velocity field $v^i(x, \tau)$ defined at a conformal time $\tau \equiv \int dt/a(t)$. In this case the Newtonian cosmological perturbations yield an accurate description [1]. Finally, we will reduce our analysis to the case without vorticity where $\theta \equiv \partial_i v^i$. In this case, the perturbations can be written in a two-component form [2, 17],

$$\partial_\eta \Psi_a(k, \eta) + \Omega_{ab} \Psi_b(k, \eta) = \gamma_{abc}(k_1, k_2) \Psi_b(k_1, \eta) \Psi_c(k_2, \eta), \quad (2)$$

where

$$\Psi_1(k, \eta) \equiv \delta(k, \eta), \quad \Psi_2(k, \eta) \equiv -\frac{\theta(k, \eta)}{f_+(\eta)\mathcal{H}}, \quad (3)$$

and we have introduced the functions $\mathcal{H} \equiv \frac{d \ln a(\tau)}{d\tau}$ and $f_+(\eta) \equiv \frac{d \ln D_+(\eta)}{d \ln a(\eta)}$ and the time $\eta \equiv \ln D_+(\tau)$, with $D_+(\tau)$ being the linear growing mode of the density contrast

$$\delta^L(k, \tau) = D_+(\tau) \delta_0(k). \quad (4)$$

The momenta k, k_1, k_2 are vectors and the equation is understood as being summed over double indices and integrated over the two momenta k_1 and k_2 with the measure $\delta^{(3)}(k - k_1 - k_2)$ on the right-hand side. This fixes our convention for Fourier transforms. In the following we only write indices and integrations when the notation of an equation could be ambiguous.

The matrix γ constituting the mode coupling can be written in symmetric form with the elements

$$\gamma_{121} = \alpha(k_1, k_2)/2, \quad \gamma_{112} = \alpha(k_2, k_1)/2, \quad \gamma_{222} = \beta(k_1, k_2), \quad (5)$$

with

$$\alpha(k_1, k_2) \equiv \frac{(k_1 + k_2) \cdot k_1}{k_1^2}, \quad \beta(k_1, k_2) \equiv \frac{(k_1 + k_2)^2 k_1 \cdot k_2}{2k_1^2 k_2^2}, \quad (6)$$

and all other elements vanishing.

In the case where one of the momenta flowing into the vertex is soft ($k_1 \ll k$ or $k_2 \ll k$) the previous vertex reduces to

$$\gamma_{ijk} \rightarrow \delta_{j2} \delta_{ik} \frac{k_2 \cdot k_1}{2k_1^2} + \delta_{k2} \delta_{ij} \frac{k_2 \cdot k_1}{2k_2^2}. \quad (7)$$

¹Deviations from this assumption can be taken into account by using the effective language of [15] (see also [16]). Since we focus on the first non-linear effects those deviations are not important for our results.

The matrix Ω depends on the underlying cosmology and can depend on the conformal time η (but not on momentum). It may also contain information about modifications of gravity [9]. Remarkably, our main results will be valid for any Ω . For completeness let us remind that in a flat matter-dominated Einstein-de Sitter Universe for which $\Omega_m = 1$ and $D_+(\tau) = a(\tau)$ it reads

$$\Omega = \begin{pmatrix} 0 & -1 \\ -3/2 & 1/2 \end{pmatrix}. \quad (8)$$

Note also that the common Zel'dovich approximation [18] differs from the exact dynamics (2) only by the choice of the Ω -matrix [2, 19, 20]

$$\Omega^{ZA} = \begin{pmatrix} 0 & -1 \\ 0 & -1 \end{pmatrix}. \quad (9)$$

The equations (2) can be solved perturbatively by treating the right side of the equation that mixes modes with different momentum as a perturbation to the linear equation

$$\partial_\eta \Psi^L(k, \eta) + \Omega(\eta) \Psi^L(k, \eta) = 0. \quad (10)$$

This perturbative scheme, known as standard perturbation theory or SPT, is based on the assumption that the amplitude of the perturbations Ψ is small. The solution to the previous equation can be easily written in term of the Green's function and the initial conditions $\Psi(k, \eta_0)$ as

$$\Psi^L(k, \eta) = e^{-\int_{\eta_0}^{\eta} d\bar{\eta} \Omega(\bar{\eta})} \Psi(k, \eta_0) \Theta(\eta - \eta_0) \equiv g(\eta, \eta_0) \Psi(k, \eta_0), \quad (11)$$

where we used the notation $\Theta(x)$ for the Heaviside step function to avoid confusion with the velocity field θ . If the matrix Ω is independent of η , the Green's function depends only on the difference $\eta - \eta_0$. For the case (8), its explicit form is

$$g(\eta, \eta_0) = \frac{e^{(\eta - \eta_0)}}{5} \begin{pmatrix} 3 & 2 \\ 3 & 2 \end{pmatrix} \Theta(\eta - \eta_0) + \frac{e^{-3(\eta - \eta_0)/2}}{5} \begin{pmatrix} 2 & -2 \\ -3 & 3 \end{pmatrix} \Theta(\eta - \eta_0), \quad (12)$$

from where we can readily identify the growing and the decaying mode. The solution to the equation (2) can formally be written as

$$\begin{aligned} \Psi_a(k, \eta) &= g_{ab}(\eta, \eta_0) \Psi_b(k, \eta_0) \\ &+ \int_{\eta_0}^{\eta} g_{ab}(\eta, \bar{\eta}) \gamma_{bcd}(k_1, k_2) \Psi_c(k_1, \bar{\eta}) \Psi_d(k_2, \bar{\eta}). \end{aligned} \quad (13)$$

The perturbative solution (in powers of $\Psi_a(k, \eta_0)$) can then be obtained by successively reinserting the left-hand side into the previous integral. Physical observables can be evaluated by performing statistical averages over these fields. A particularly useful one is the power spectrum given by

$$\langle \Psi_a(k_1, \eta) \Psi_b(k_2, \eta) \rangle \equiv \delta^{(3)}(k_1 + k_2) P_{ab}(k_1, \eta). \quad (14)$$

The conservation of momentum in the mode coupling term ensures that the two point correlator (14) is proportional to the delta function at all times. This reflects the translation invariance of the system. The leading order contribution to it in SPT is the so-called linear power spectrum

$$P_{ab}^L(\eta) \equiv g_{ac}(\eta, \eta_0) g_{bd}(\eta, \eta_0) P_{cd}^0(k), \quad (15)$$

where we have introduced the initial power spectrum

$$\langle \Psi_a(k_1, \eta_0) \Psi_b(k_2, \eta_0) \rangle \equiv \delta^{(3)}(k_1 + k_2) P_{ab}^0(k_1). \quad (16)$$

Thus,

$$P_{ab}(k, \eta) = P_{ab}^L(\eta) + \dots. \quad (17)$$

In the following we only deal with Gaussian initial conditions that are uniquely specified by the initial power spectrum $P^0(k)$.

The perturbative expansion can be pictorially represented by classical Feynman rules [3]. The two building blocks are the vertex and the Green's function displayed in Fig. 1. The causal structure of the integral (13) enforces a flow of time that is indicated by the arrow. The initial power spectrum is indicated by a box. The leading topologies that contribute to the power spectrum are shown in Fig. 2.

3 Renormalized perturbation theory and the eikonal approximation

In this section we briefly review the key aspects of renormalized cosmological perturbations (RPT) [3, 4] (see also [21, 22] for similar resummations in the case of fluid dynamics) and the eikonal approach [13] which constitute the

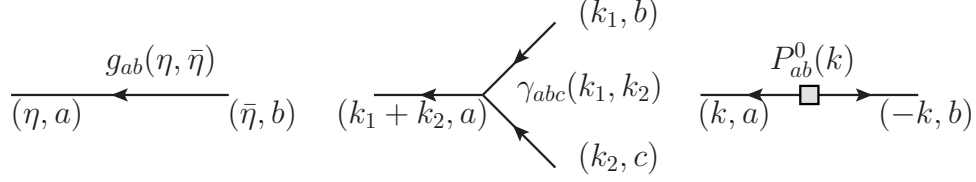


Figure 1: Building blocks of the Feynman rules of standard perturbation theory.

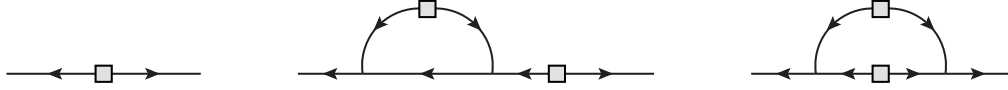


Figure 2: All tree level and one-loop contributions to the power spectrum.

basis for our later discussions. Both schemes are motivated to address convergence issues related to the enhancement of the vertex (coupling) between hard and soft modes. For example, the diagram in Fig. 3 scales for $k \gg q$ as

$$g_{ab}(\eta, \eta_0) \int_{\eta_0}^{\eta} d\bar{\eta} \int_{\eta_0}^{\bar{\eta}} d\tilde{\eta} g_{2c}(\bar{\eta}, \eta_0) g_{2d}(\tilde{\eta}, \eta_0) \int d^3q \frac{(k \cdot q)^2}{q^4} P_{cd}^0(q). \quad (18)$$

So even if the final integral is finite and the growing of the Green's function small, there results an enhancement from attaching more soft loops to a line with momentum k if k is large enough, i.e. if $k \sigma_d \gg 1$, where

$$\sigma_d^2(\Lambda, \eta) \equiv \frac{1}{k^2} \int^{\Lambda} d^3q \frac{(k \cdot q)^2}{q^4} P^L(q, \eta) = \frac{4\pi}{3} \int^{\Lambda} dq P^L(q, \eta), \quad (19)$$

where $P^L \equiv P_{22}^L$ and Λ represents the scale at which we cut-off the initial power spectrum. This is precisely the scale of non-linearity discussed in the introduction, Eq. (1). In particular, $k^2 \sigma_d^2$ can be larger than the dimensionless variance of the density field [12]

$$\sigma_l^2(\Lambda, \eta) \equiv 4\pi \int^{\Lambda} dq q^2 P^L(q, \eta), \quad (20)$$

which would control the non-linear scale in the absence of vertex enhancement². At this stage it seems that to describe physics beyond the scale σ_d

²We chose the notation for these two quantities that best adapts to previous literature. We also define $\sigma_{d,l}(\Lambda) \equiv \sigma_{d,l}(\Lambda, \eta = 0)$ for the values today, and $\sigma_d \equiv \sigma_d(\Lambda \rightarrow \infty)$;

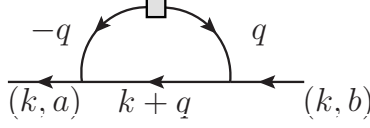


Figure 3: One-loop contribution to the propagator.

one should first be able to sum up all soft contributions to the propagation of hard modes. Once this is done, one expects to find a perturbation theory with better convergence properties. This idea was put on a firm basis in the theory of RPT [3, 4]. In this case, the role of the Green's function (12) in the Feynman rules is played by the *propagator*

$$G_{ab}^{(1)}(k, \eta, \bar{\eta}) \delta^{(3)}(k - k_1) \equiv \left\langle \frac{\delta \Psi_a(k, \eta)}{\delta \Psi_b(k_1, \bar{\eta})} \right\rangle, \quad (21)$$

that in terms of perturbation theory contains all diagrams with exactly one incoming and one outgoing line and arbitrary (soft or not) loop corrections to it ³.

As we will review in the next section, the leading behavior for large momenta k (and considering only the contribution from the growing mode) can be resummed for the propagator of renormalized perturbation theory [3]

$$G_{RPT}^{(1)}(k, \eta, \bar{\eta}) = g_{ab}(\eta, \bar{\eta}) \exp \left(-\frac{1}{2} k^2 \sigma_d^2 (a(\eta) - a(\bar{\eta}))^2 \right), \quad (22)$$

where we used $a(\eta) \simeq e^\eta$ and set $a = 1$ today.

The perturbative expansion in RPT can be formulated by means of the n -point propagators defined as [23]

$$G_{aa_i \dots a_n}^{(n)}(k_i, \eta, \bar{\eta}) \delta^{(3)}(k - \sum k_i) \equiv \frac{1}{n!} \left\langle \frac{\delta^n \Psi_a(k, \eta)}{\delta \Psi_{a_1}(k_1, \bar{\eta}) \dots \delta \Psi_{a_n}(k_n, \bar{\eta})} \right\rangle. \quad (23)$$

In terms of those, the power spectrum at late times can be written as

$$\begin{aligned} P_{ab}(k, \eta) &= \sum_n n! \left(\prod_{i=1}^n \int d^3 k_i P_{a_i b_i}^0(k_i) \right) \delta^{(3)}(k - \sum k_i) \\ &\quad \times G_{aa_1 \dots a_n}^{(n)}(k_i, \eta, \eta_0) G_{bb_1 \dots b_n}^{(n)}(-k_i, \eta, \eta_0). \end{aligned} \quad (24)$$

note that this limit exists for realistic power spectra. In contrast, $\sigma_l(\Lambda)$ has a logarithmic sensitivity to Λ , as will be discussed in detail in section 7.

³The meaning of the superscript (1) is clarified below.

Pictorially, $G^{(n)}$ is the sum of all diagrams with n incoming lines and one outgoing line. As long as the resummed n -point functions $G^{(n)}$ are well behaved for large k , the sum should converge. It was shown in [23] that the corrections from soft modes to the individual n -point propagators also generate an exponential suppression related to the scale σ_d .

For the power spectrum and related observables, the previous results provide only a partial resummation of the effects of soft modes. This is commonly encoded in an expression of the form (compare with (17))

$$P = \left(G_{RPT}^{(1)}\right)^2 P^0 + P_{MC}, \quad (25)$$

where the piece P_{MC} contains all the contributions from other diagrams. From the previous arguments, one may expect P_{MC} to be better behaved than the corrections in Eq. (17) and that RPT with the leading effect of the soft modes to the propagator resummed have better convergence properties than SPT.

To check this, one needs to deal with *all* soft corrections to the hard skeletons behind observables. This is the purpose of the eikonal approximation [13]. The main observation of this approach is that in (2) the contribution from the soft modes to the mode coupling is approximated by

$$\begin{aligned} \int d^3 k_1 d^3 k_2 \gamma_{abc}(k_1, k_2) \Psi_b(k_1, \eta) \Psi_c(k_2, \eta) \delta^{(3)}(k - k_1 - k_2) \\ \simeq \Psi_a(k, \eta) \int d^3 q \frac{k \cdot q}{q^2} \Psi_2(q, \eta). \end{aligned} \quad (26)$$

Using this relation in (2) leads to the result (cf. (11))

$$\Psi(k, \eta) = g(\eta, \eta_0) \exp \left[\int_{\eta_0}^{\eta} d\tilde{\eta} \int d^3 q \frac{k \cdot q}{q^2} \Psi_2(q, \tilde{\eta}) \right] \Psi(k, \eta_0). \quad (27)$$

In turn, for the propagator (21) in the eikonal approximation this yields

$$G_{\text{eikonal}}^{(1)}(k, \eta, \bar{\eta}) = g(\eta, \bar{\eta}) \left\langle \exp \left[\int_{\bar{\eta}}^{\eta} d\tilde{\eta} \int d^3 q \frac{k \cdot q}{q^2} \Psi_2(q, \tilde{\eta}) \right] \right\rangle, \quad (28)$$

that for Gaussian initial conditions is (in leading order, see (11)) given by the second cumulant

$$G_{\text{eikonal}}^{(1)}(k, \eta, \bar{\eta}) = g(\eta, \bar{\eta}) \exp \left(\frac{c_2}{2} \right), \quad (29)$$

with

$$\begin{aligned}
c_2 &\equiv \left\langle \left(\int_{\bar{\eta}}^{\eta} d\tilde{\eta} \int d^3q \frac{k \cdot q}{q^2} \Psi_2(q, \tilde{\eta}) \right)^2 \right\rangle_{connected} \\
&\simeq - \int_{\bar{\eta}}^{\eta} d\hat{\eta} d\tilde{\eta} g_{2a}(\hat{\eta}, \eta_0) g_{2b}(\tilde{\eta}, \eta_0) \int d^3q \frac{(k \cdot q)^2}{q^4} P_{ab}^0(q).
\end{aligned} \tag{30}$$

To compare it with (22), we consider only the growing mode, for which

$$c_2 = -k^2 \sigma_a^2 (a(\eta) - a(\bar{\eta}))^2, \tag{31}$$

which shows that the eikonal approximation indeed resums the leading soft corrections. A possible physical interpretation of this propagator is that the modes of hard momentum k are scattered by the background of soft modes. This decorrelates the modes over time what leads to the exponential fall-off of the propagator for late times.

One of the advantages of the eikonal approximation is that it allows to go beyond the propagator and compute the effects of the soft modes in the power spectrum [13]. Since the exponent in (27) is odd under a sign flip of k and the power spectrum involves the combination $\langle \Psi(k) \Psi(k') \rangle \propto \delta(k + k')$, the two exponential factors cancel and the resulting power spectrum is unsuppressed. Hence, the complete resummation of the leading effect of soft modes does not produce an expression as (25) (see also (24)), but leaves the power spectrum (17) unchanged [13]. This result can also be derived in the diagrammatic language of RPT, which we do in the next section.

4 Resummation of general skeleton diagrams

Let us start this section by reviewing the resummation of the leading contributions to the propagator as first given in [3]. We want to resum all leading soft corrections in the limit of large k . A vertex with one soft and one hard incoming mode is enhanced by a factor $k \cdot q/q^2$, while a vertex with two similar modes is not enhanced. Hence, for fixed loop order the dominant contribution comes from attaching all soft modes directly to the hard mode that flows through the linearized propagator. Possible diagrams at one and two loop order are shown in Figs. 3 and 4. In the limit of soft corrections, the vertex is proportional to the Kronecker delta (7). The inflowing momentum can be neglected at leading order and the Green's functions $g(\eta_{i+1}, \eta_i)$

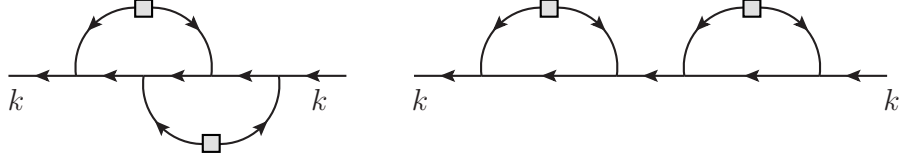


Figure 4: Two-loop contributions to the propagator.

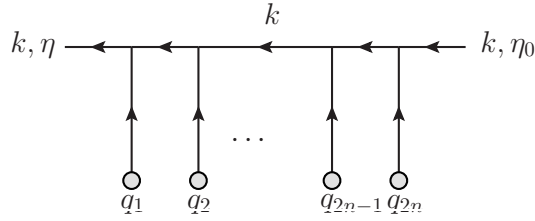


Figure 5: Soft modes attached to a hard linearized propagator. If the inflow of momentum is neglected, the order of the vertices is irrelevant.

along the hard mode combine to one linearized propagator involving only the very first and the very last time, $g(\eta, \eta_0)$. This is a generic result that hinges on the group structure of the propagators. In particular it is valid for any expansion history of the Universe and beyond the restriction to the growing mode case. A diagram with n loops involves attaching $2n$ linearized propagators of the form depicted in Fig. 5. As long as the inflow of soft momentum is neglected, the order of all the vertices is irrelevant. The time integrations involves (with $\eta_{2n+1} \equiv \eta$)

$$\prod_{i=0}^{2n} \int_{\eta_0}^{\eta_{i+1}} d\eta_i g_{2a}(\eta_i, \eta_0). \quad (32)$$

Since we are considering the effect of all possible contractions with the initial power spectrum, the symmetries of the resulting expressions allow us to rewrite the time integrations as

$$\frac{1}{(2n)!} \prod_{i=0}^{2n} \int_{\eta_0}^{\eta} d\eta_i g_{2a}(\eta_i, \eta_0). \quad (33)$$

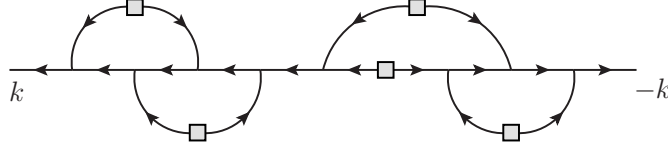


Figure 6: A contribution to the power spectrum at four-loop order with $n_{ll} = 2$, $n_{lr} = 1$ and $n_{rr} = 1$.

In total, there are $(2n-1)!!$ possibilities to contract the soft modes with initial power spectra. Thus, at n -loop order one finds a contribution $(c_2/2)^n/n!$ and summing over loops the eikonal result (29) is recovered. Notice that this result is valid for any matrix Ω , which just changes the form of the linearized propagator and hence the particular value of σ_d .

4.1 Power Spectrum

Next, we consider all soft corrections to the power spectrum. A generic graph at four-loop order is shown in Fig. 6. Imagine there are n_{ll} loop corrections to the left hard linearized propagator and n_{rr} loop corrections to the right linearized hard propagator. In addition, we denote the number of soft loop corrections connecting the left linearized hard propagator with the right one by n_{lr} . Following the same logic that applied for the propagator, one can extend all time integrations from η_0 to η what leads to a factor $1/(2n_{ll} + n_{lr})!$ for the left linearized hard propagator and $1/(2n_{rr} + n_{lr})!$ for the right one. There are $\binom{2n_{ll} + n_{lr}}{n_{lr}}$ combinations to split the soft modes connected to the left branch into the two groups, such that the combinatorial factor before contraction is $1/(2n_{ll})!n_{lr}!$ and similarly for the right soft modes one finds $1/(2n_{rr})!n_{lr}!$. As before, there are $(2n_{ll} - 1)!!$ possibilities to contract the left loops and $(2n_{rr} - 1)!!$ to contract the right ones. In addition there are $n_{lr}!$ combinations to contract the left modes with the right ones. Finally, notice that the left and right loops produce a factor c_2 while the soft loops connecting the left branch with the right one leads to a factor $-c_2$. In summary, one finds that the leading corrections from soft modes for the power spectrum of a hard mode reduce to the factor

$$\sum_{n_{ll}, n_{lr}, n_{rr}} \frac{1}{n_{ll}!n_{lr}!n_{rr}!} \left(\frac{c_2}{2}\right)^{n_{ll}} \left(\frac{c_2}{2}\right)^{n_{rr}} (-c_2)^{n_{lr}} = e^{c_2/2 - c_2 + c_2/2} = 1. \quad (34)$$

Thus, the corrections that connect the different branches exactly compensate for the exponential suppression from resumming the soft corrections to the propagators. This is in complete accord with the eikonal approximation that predicts a suppression in the propagator but not in the power spectrum. This cancellation of the leading soft corrections to the power spectrum was first observed in [11]. Here we gave a diagrammatic derivation (cf. also [10, 24]).

The previous result implies that the expansion (24) does not necessarily improve the convergence in the power spectrum compared to standard perturbation theory (see [26] for similar conclusions in the context of RegPT). According to the above resummation, in the limit where all k_i but one momentum are soft the n -point functions $G^{(n)}$ are enhanced such that the sum produces an exponential that cancels the exponential suppression in each of the $G^{(n)}$ observed in RPT [23]. Parametrically, the leading soft corrections to the different contributions to the sum (24) with resummed n -point propagators scale as $P \sim \sum_n \frac{1}{n!} (k \sigma_d(\eta))^{2n} \exp(-k^2 \sigma_d(\eta)^2)$. So for large $k^2 \sigma_d(\eta)^2 \gg 1$, the sum can only start converging after $n \simeq k^2 \sigma_d(\eta)^2$ terms are taken into account. In fact the situation is even worse, since reproducing the leading k -behavior order by order is not enough to ensure the cancellation of subleading terms in the regime of large k as we show below.

4.2 General Skeleton

The soft corrections to arbitrary skeletons of hard modes can also be resummed. For example consider any of the one-loop contributions to the power spectrum depicted in Fig. 2 in a regime where none of the involved momenta is soft. The diagram involves several linearized propagators with momenta k_i . Soft loops can connect arbitrary linearized propagators and we denote the according number as n_{ij} . The total number of soft lines at a linearized propagator i is then $N_i = 2n_{ii} + \sum_{j \neq i} n_{ij}$. As before, the soft lines are time ordered and extending the time integrations over the full range leads to a factor $1/N_i!$. The full range is hereby given by the time the original linearized propagator in the skeleton diagram depends on that we denote η_i and $\bar{\eta}_i$. Splitting the soft lines into groups yields several binomial factors that contribute factors of the form $1/(2n_{ii})!/\prod_{j \neq i} n_{ij}!$. This is valid for an arbitrary skeleton of hard modes.

Connecting a soft line of a linearized propagator i with a soft line of a

linearized propagator j gives the integral

$$- \int d^3q \frac{k_i \cdot q}{q^2} \frac{k_j \cdot q}{q^2} P_{ab}^0(q), \quad (35)$$

and the time dependence⁴

$$\int_{\tilde{\eta}_i}^{\eta_i} d\tilde{\eta} g_{2a}(\tilde{\eta}, \eta_0) \int_{\tilde{\eta}_j}^{\eta_j} d\hat{\eta} g_{2b}(\hat{\eta}, \eta_0). \quad (36)$$

With the corresponding combinatorial factor to connect soft lines, the final correction to the diagram reads

$$\exp \left[-\frac{1}{2} \int d^3q Y_{2a} Y_{2b} P_{ab}^0(q) \right], \quad (37)$$

with

$$Y_{ab} \equiv \sum_i \int_{\tilde{\eta}_i}^{\eta_i} d\tilde{\eta} \frac{k_i \cdot q}{q^2} g_{ab}(\tilde{\eta}, \eta_0). \quad (38)$$

This result is actually expected from the eikonal approximation as we will see in the next section.

Depending on the skeleton diagram, the function Y_{ab} can be further simplified. Consider two linearized propagators that originate from two initial power spectra and end in a common vertex. The two corresponding contributions to Y_{ab} then share the same range of time integration and can be combined to one contribution that is proportional to the sum of the two momenta of the skeleton diagram. Hence, this term can also be combined with the subsequent propagator. An illustration of this is given in Fig. 7. This fragment of a diagram acquires through soft corrections the contribution

$$\begin{aligned} Y_{ab} &\ni \int_{\eta_0}^{\eta_1} d\tilde{\eta} \frac{k_1 \cdot q}{q^2} g_{ab}(\tilde{\eta}, \eta_0) + \int_{\eta_0}^{\eta_1} d\tilde{\eta} \frac{k_2 \cdot q}{q^2} g_{ab}(\tilde{\eta}, \eta_0) \\ &\quad + \int_{\eta_1}^{\eta_2} d\tilde{\eta} \frac{(k_1 + k_2) \cdot q}{q^2} g_{ab}(\tilde{\eta}, \eta_0) \\ &= \int_{\eta_0}^{\eta_2} d\tilde{\eta} \frac{(k_1 + k_2) \cdot q}{q^2} g_{ab}(\tilde{\eta}, \eta_0). \end{aligned} \quad (39)$$

⁴ Note that, since time has to increase along the arrows of each linearized propagator, cf. (12), the time $\tilde{\eta}$ of a soft vertex that is attached between vertices at $\tilde{\eta}_i$ and η_i has to lie within the time interval $\tilde{\eta}_i < \tilde{\eta} < \eta_i$.

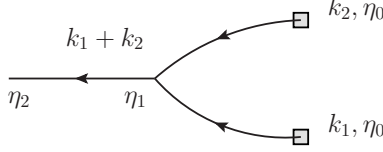


Figure 7: An example of several contributions to Y_{ab} that can be combined.

Remarkably, the functions Y_{ab} vanish for any equal-time correlator as for example the power spectrum and the bispectrum.

We will see in the next section that this will allow us to go beyond the leading order considered in previous analysis [11, 13] and show that the effects of soft modes over hard modes k produce at most an enhancement of $\log k$ compared to the linear power spectrum any order in perturbation theory.

5 Eikonal approximation - the higher orders

In this section we extend the previous results and show that also subleading soft corrections cancel each other in equal-time correlators. This is done by using the eikonal approximation [11, 13] as the zeroth order and systematically expanding the evolution equations around the eikonal limit. As has been shown in [13], the eikonal approximation can be represented on the level of the equations of motion by introducing a filter function that separates hard from soft modes, and rewriting (2) as

$$\partial_\eta \Psi_a(k, \eta) + \Omega_{ab} \Psi_b(k, \eta) = 2F_\epsilon(k_1, k) \tilde{\gamma}_{abc}(k_1, k_2) \Psi_b(k_1, \eta) \Psi_c(k, \eta) + \{\gamma_{abc} \Psi_b \Psi_c\}_H, \quad (40)$$

where we used the notation

$$\tilde{\gamma}_{abc}(k_1, k_2) \equiv \delta_{b2} \delta_{ac} \frac{k_1 \cdot (k_1 + k_2)}{2k_1^2}. \quad (41)$$

The function F_ϵ is a filter that distinguishes soft modes from hard modes, for example the Heaviside step-function $F_\epsilon(k_1, k) = \Theta(\epsilon|k| - |k_1|)$. In the previous construction the term $\{\dots\}_H$ denotes the difference between the full interaction term (2) and the first term. Only the first term on the right side becomes large in the limit $|k_1| \ll |k|$. The eikonal approximation is

obtained by neglecting the term $\{\dots\}_H$. The remaining term can then be resummed and absorbed into the Green's function

$$\begin{aligned} g_{eikonal}(k, \eta, \eta_0) &\equiv g(\eta, \eta_0) \exp \left[\int_{\eta_0}^{\eta} d\tilde{\eta} \int d^3q F_{\epsilon}(q, k) \frac{k \cdot q}{q^2} \Psi_2(q, \tilde{\eta}) \right] \\ &\equiv g(\eta, \eta_0) \xi(k, \eta, \eta_0). \end{aligned} \quad (42)$$

To discuss the cancellation of subleading terms it is necessary to discuss the rest term $\{\dots\}_H$ in some detail. To this aim we add and subtract several terms to the right-hand side of (2), and write the rest term in the form⁵

$$\begin{aligned} \{\gamma_{abc} \Psi_b \Psi_c\}_H &\equiv 2F_{\epsilon}(k_1, k) \tilde{\gamma}_{abc}(k_1, k_2) \Psi_b(k_1, \eta) (\Psi_c(k_2, \eta) - \Psi_c(k, \eta)) \\ &\quad + F_{\epsilon}(k_1, k) (\gamma_{abc}(k_1, k_2) - \tilde{\gamma}_{abc}(k_1, k_2)) \Psi_b(k_1, \eta) \Psi_c(k_2, \eta) \\ &\quad + F_{\epsilon}(k_2, k) (\gamma_{abc}(k_1, k_2) - \tilde{\gamma}_{acb}(k_2, k_1)) \Psi_b(k_1, \eta) \Psi_c(k_2, \eta) \\ &\quad + (1 - F_{\epsilon}(k_1, k) - F_{\epsilon}(k_2, k)) \gamma_{abc}(k_1, k_2) \Psi_b(k_1, \eta) \Psi_c(k_2, \eta). \end{aligned} \quad (43)$$

To go beyond the leading corrections we use the eikonal approximation as the zeroth order solution and treat each of the remaining terms in (43) perturbatively as an effective vertex. The particular splitting into these four terms ensures that each diagram constructed in this scheme is free of any (residual) enhancement from soft modes (this will be discussed in more detail below).

The calculation of averaged quantities at a given order involves mixed cumulants of the field due to the exponentiation of soft fields in (42). At leading order in the soft background field, these cumulants reproduce the Y functions (38) appearing in (37) [13].

The perturbative expansion defined out of (43) with the propagator (42) seems better behaved than the one of SPT. This is because it tames the effects related to the scale (19). This advantage would justify its use despite its higher degree of complexity coming from the proliferation of vertices⁶ and the appearance of mixed cumulants mentioned above. But the results from the previous section show that the leading effect in σ_d cancels for equal-time correlators and suggest that this may be a spurious scale. We are now

⁵Recall that a term $\delta^{(3)}(k_1 + k_2 - k)$ and integrations in k_1 and k_2 are present in all the non-linear terms.

⁶ In particular some of the terms that have been added and subtracted in (43) are not translation invariant, which leads to an apparent violation of momentum conservation in individual vertices and a perturbative expansion where single contributions to the power spectrum are non-diagonal in momentum space (although the full theory still respects translation invariance).

going to prove this for all subleading effects. Thus, for these observables the convergence of any scheme based on resumming the effects related to (19) cannot be better than SPT.

We support this claim by interpreting the split of (43) in terms of diagrams. In any diagram, the putative enhancement at scales $k \sigma_d \gg 1$ is related to soft momenta dressing a hard skeleton with momenta of order k . In the previous section, we showed that the leading effect (which at n -loop order scale as $(k \sigma_d)^{2n}$) cancels. To prove the cancellation of the subleading terms down to order $\mathcal{O}(k^0)$, we need to use the perturbation theory based on (43). In comparison to the eikonal limit this requires to account for the momentum injected into the diagram from the soft loops, for the full vertex compared to (41) and finally for the self-coupling of soft modes (i.e. soft modes coupled to other soft modes). Notice first that the vertices coming from the last three terms in (43) do not produce any enhancement and can be treated perturbatively. The self-coupling of the soft modes is in (43) represented by the fact that we resum the time-dependent contribution $\Psi(q, \eta)$ (the whole non-linear form). Whenever this propagator is used for vertices that conserve momentum, the phase will disappear. Thus, the only place where the scale σ_d may appear is in the term that does not conserve momentum,

$$2F_\epsilon(k_1, k) \tilde{\gamma}_{abc}(k_1, k_2) \Psi_b(k_1, \eta) (\Psi_c(k_2, \eta) - \Psi_c(k, \eta)). \quad (44)$$

If $k_1 \ll k$, the vertex is enhanced but the contribution comes with a factor⁷

$$\begin{aligned} (\Psi(k_2, \eta) - \Psi(k, \eta)) &\simeq g(\eta, \eta_0) \xi(k_2, \eta, \eta_0) \\ &\times [\Psi(k_2, \eta_0) - \Psi(k, \eta_0) \xi(k - k_2, \eta, \eta_0)] . \end{aligned} \quad (45)$$

For equal-time correlators the factor $\xi(k_2, \eta, \eta_0)$ will combine with the remaining factors of the diagram to yield unity, while the second term in brackets is not enhanced in k any more and can be treated perturbatively (recall the factor $F_\epsilon(k_1, k)$ in (44))

$$\xi(k - k_2, \eta, \eta_0) = \xi(k_1, \eta, \eta_0) \simeq 1 + \int_{\eta_0}^{\eta} \int d^3 q \frac{k_1 \cdot q}{q^2} \Psi_2(q, \eta) . \quad (46)$$

Hence, $(\Psi(k_2, \eta) - \Psi(k, \eta))$ is of order k_1/k , which cancels the enhancement coming from $\tilde{\gamma}$, and the factors $\xi(k, \eta, \eta_0)$ also cancel in this vertex.

⁷This expression is precise to order $\mathcal{O}(\epsilon)$.

This proves that the enhancement from soft modes characterized by the scale σ_d is completely absent in equal-time observables. This includes the matter power spectrum and any other n -point correlation function, like the bispectrum. Notice that the argument in this section is rather general. The main assumption is that the leading term in (43) can be treated non-perturbatively and that the resulting cumulants are not enhanced for large k . Another assumption is that the Gaussian random field $\Psi(k)$ can be expanded in a Taylor series, see also [11]. On the other hand, the precise form of the vertices is irrelevant for the argument to work as far as the full vertices respect translation invariance and provided that the soft-enhanced terms are proportional to the unit matrix $\tilde{\gamma}_{abc} \propto \delta_{ac}$ such that ξ has no matrix structure. The latter condition is for example violated in a multi-component fluid for the non-adiabatic decaying isodensity modes [14]. Notice also that, since the proof does not rely on the form of the linear part Ω (given by (8) for Einstein-de Sitter), it is true for any cosmological expansion history, including any possible term that modifies the linear term. This means that it is valid as well for the Zel'dovich approximation (9), in accordance with [12].

In the next section we complement the general proof presented above by an explicit check of the cancellation for the matter power spectrum in an Einstein-de Sitter cosmology at two-loop order, and for the loop integrand up to four-loop order.

6 Matter power spectrum

In this section we want to clarify the consequences of the cancellation of subleading corrections related to the scale σ_d for the matter power spectrum. The absence of physical effects related to the scale σ_d was already derived at leading order and all loops for the matter power spectrum in [11]. This was interpreted in [12] as a consequence of Galilean invariance (see [24] for a recent discussion). In [12, 27] the explicit calculation for the matter power spectrum and bispectrum to two loops and with scale invariant initial power spectrum was performed, and no enhancement was found (the corrections are related to the scale σ_l). Note that for scale-invariant initial spectra with a power-law index smaller than -1 the cancellation of soft corrections is closely related to the cancellation of infrared divergences [12].

Even if our proof of section 5 for the absence of enhancement by soft modes is valid for any initial power spectrum, in this section we will work

with a realistic Λ CDM form. For this, an analytic expression is given by the prominent fit by Eisenstein and Hu [28]. For analyzing the leading asymptotic behavior of loop corrections, it is often sufficient to consider the restriction of this fit to the Einstein-de Sitter case with spectral index $n_s = 1$,

$$P^0(k, \eta_0) \sim \alpha \frac{k L^2}{(L + C\beta^2 k^2)^2}, \quad (47)$$

with

$$L \equiv \ln(e + 1.84\beta k), \quad C \equiv 14.4 + \frac{325}{1 + 60.5(\beta k)^{1.08}}, \quad \beta \simeq 6.86 \text{ Mpc}. \quad (48)$$

For the normalization of the spectrum we fit the previous formula to the linear power spectrum at $z = 0$ found in [29], which yields $\alpha \simeq 17000 \text{ Mpc}^4$. Note that, for our numerical analysis, we use as input a linear power spectrum obtained with CAMB for WMAP5 parameters as provided in [29] (see the footnote 10 for the effect of considering $n_s \neq 1$).

6.1 Formalism

The different contributions to the power spectrum in standard perturbation theory at n -loop order can be written schematically as

$$\begin{aligned} P_{n-loop}(k, \eta) &= \sum_{m=1}^{n+1} \int d^3 k_1 \dots d^3 k_{n+1} A_m^{(n)}(k_1, \dots, k_{n+1}) \\ &\times P^L(k_1, \eta) \dots P^L(k_{n+1}, \eta) \delta^{(3)}(k - k_1 \dots - k_m). \end{aligned} \quad (49)$$

For example at one-loop level, the two diagrams in Fig. 2 involve the spectral dependence $P^0(k) P^0(q)$ and $P^0(k - q) P^0(q)$, which corresponds to $m = 1$ and $m = 2$, respectively (as well as $q \equiv k_2$). Those diagrams are related to the terms denoted by⁸ P_{13} and P_{22} in the standard perturbation theory [2]. The expression of $A_m^{(n)}$ in terms of the symmetrized kernels $F_n(k_1, \dots, k_n)$ that characterize the non-linear evolution of the density field in the growing mode in an Einstein-de Sitter Universe [2, 27, 30] is shown in Eq. (77).

We are interested in the case where the momentum k is much larger than the scale σ_d^{-1} . In this case, the previous integral seems to be dominated by the

⁸These quantities P_{IJ} have nothing to do with the quantities P_{ab} introduced above. It is always clear from the context to which quantity we refer.

regime in which all but one of the modes k_i are soft. This happens because the $A_m^{(n)}$ are homogeneous rational functions in the momenta and in the previous regime the largest enhancement is of order $A_m^{(n)} \propto \prod_i (k \cdot k_i / k_i^2)^2 \propto |k|^{2n}$. Furthermore, the steep fall-off of the power spectrum (47) at high k implies that the regime $k \sigma_d \gg \sigma_l(k)$ exists. Thus, we may concentrate on the nonlinearities associated to σ_d . The results in the previous section imply that this is a naive expectation: there must be a cancellation between different terms that eliminate this effect. To find this cancellation at different loop orders, we first use the Dirac-delta function to perform the integration over k_1 in (49). For large k , enhanced contributions from soft modes would originate from the domain $|k_i| \ll |k|$ for $i = 2, \dots, n+1$ and $k_1 \simeq k$ (possible ambiguities in choosing the hardest momentum to be k_1 are taken into account by including appropriate Heaviside functions and combinatorial factors; see Appendix A for details). In order to isolate these terms, we Taylor expand

$$P^L(k_1, \eta) \Big|_{k_1=k-k_2 \dots -k_m} = \sum_{l=0} b_l(k, q) [k \partial_k]^l P^L(k, \eta), \quad (50)$$

where $q \equiv k_2 + \dots + k_m$. The coefficients scale as $b_l \propto (|q|/|k|)^l$. Therefore, since the $A_m^{(n)}$ grow as $|k|^{2n}$, we need to expand up to $l \leq 2n$ to capture all terms that can potentially be affected by enhancement for large k . By collecting all terms arising from the l -th term in the Taylor expansion, and relabelling the momenta, the n -loop power spectrum for large k can be written in the form

$$P_{n-loop}(k, \eta) \rightarrow \sum_{l \leq 2n} \int d^3 k_1 \dots d^3 k_n B_l^{(n)}(k, k_1, \dots, k_n) \times [k \partial_k]^l P^L(k, \eta) P^L(k_1, \eta) \dots P^L(k_n, \eta), \quad (51)$$

up to terms that are suppressed by the hard external momentum, $\mathcal{O}(k_i/k)$.

The $B_l^{(n)}$ are linear combinations of the $A_m^{(n)}$ for $1 \leq m \leq n+1$ multiplied by the appropriate coefficients b_l and we provide explicit expressions in Appendix A, Eq. (79). Therefore, without any cancellations, one would expect that $B_l^{(n)} \propto |k|^{2n-l}$ for large k . The results from [11] show that the leading contribution cancels, which means that the enhancement is at most $B_l^{(n)} \propto |k|^{2(n-1)-l}$. Our results of the previous section imply that this cancellation is also valid for the subleading terms and that

$$B_l^{(n)}(k, k_1, \dots, k_n) \rightarrow C_l^{(n)}(k_1, \dots, k_n) + \mathcal{O}(k_i/k), \quad (52)$$

where $B_l^{(n)}$ approaches a constant, denoted by $C_l^{(n)}$, for large k .

6.2 Results

An explicit analytical calculation showing the cancellation of k^4 - and subleading k^2 -contributions to the integrand kernels $B_l^{(n)}$ up to two loops is presented in the Appendix A. Explicit results for the asymptotic limit Eq. (52) are given in Eq. (65) and Eq. (71) for the one- and two-loop orders, respectively. In addition, we checked numerically for various momentum configurations that the cancellation of polynomially growing contributions and the asymptotic behavior Eq. (52) is indeed correct up to four loop order, see Figs. 8 and 9.

Using the analytical results Eq. (65) and Eq. (71) for the asymptotic values of the integrand kernels $B_l^{(n)}$ it is possible to derive approximate expressions⁹ (up to $O(1/k^2)$ and subleading logarithmic corrections) for the power spectrum at large k ,

$$\begin{aligned} P_{1-loop}(k) &\sim (1.14P^L(k) - 0.55k\partial_k P^L(k) + 0.1[k\partial_k]^2 P^L(k)) \sigma_l^2(k), \\ P_{2-loop}(k) &\sim (2.14P^L(k) - 1.62k\partial_k P^L(k) + 0.55[k\partial_k]^2 P^L(k) \\ &\quad - 0.082[k\partial_k]^3 P^L(k) + 0.005[k\partial_k]^4 P^L(k)) \sigma_l^4(k). \end{aligned} \quad (53)$$

From these expressions, it is clear that the expansion parameter at large k is given by powers of $\sigma_l^2(k)$. We also see that even though all the functions $B_l^{(n)}$ are of order unity, a logarithmic enhancement in the final power spectrum can arise depending on the precise shape of the initial power spectrum. For the spectrum (47) one finds¹⁰ $\sigma_l^2(k) \propto \ln^3(k)$ for large k . This is discussed in section 7. Additional enhancement can potentially come from the fact that the derivatives $(k\partial_k)^n P^L(k)$ are larger than the power spectrum $P^L(k)$ itself.

Before moving to higher loops, it is interesting to remind the behavior at small k where the linear approximation is expected to work rather well. To understand the size of loop corrections parametrically, notice that in the limit $k \rightarrow 0$, the dominating contributions to the n -loop corrections arise from the diagrams usually denoted by $P_{1,2n+1}$ and scale as $\propto k^2 P^L(k)$ (see Appendix B). The behavior of this quantity is discussed in detail in [31].

⁹We do not write explicitly the dependence on η in the rest of this section, since it is trivial to retrieve.

¹⁰For general spectral index $\sigma_l^2(k) \propto \ln^2(k)[k^{n_s-1} - k_0^{n_s-1}]/(n_s - 1)$ where $k_0 \sim 0.02 h/\text{Mpc}$. Note that for $k \ll k_* \equiv k_0 \exp(1/|n_s - 1|)$, one may safely expand in $n_s - 1$ to estimate the scaling with k . For example, $k_* \sim 10^9 h/\text{Mpc}$ for $n_s = 0.96$. All numerical results are based on the WMAP5 spectrum [29] with $n_s = 0.96$. For the analytical discussion of the limit $k \gg k_0$ it is thus legitimate to use (47) as long as $k \ll k_*$, which is very well satisfied within the regime of interest in this work.

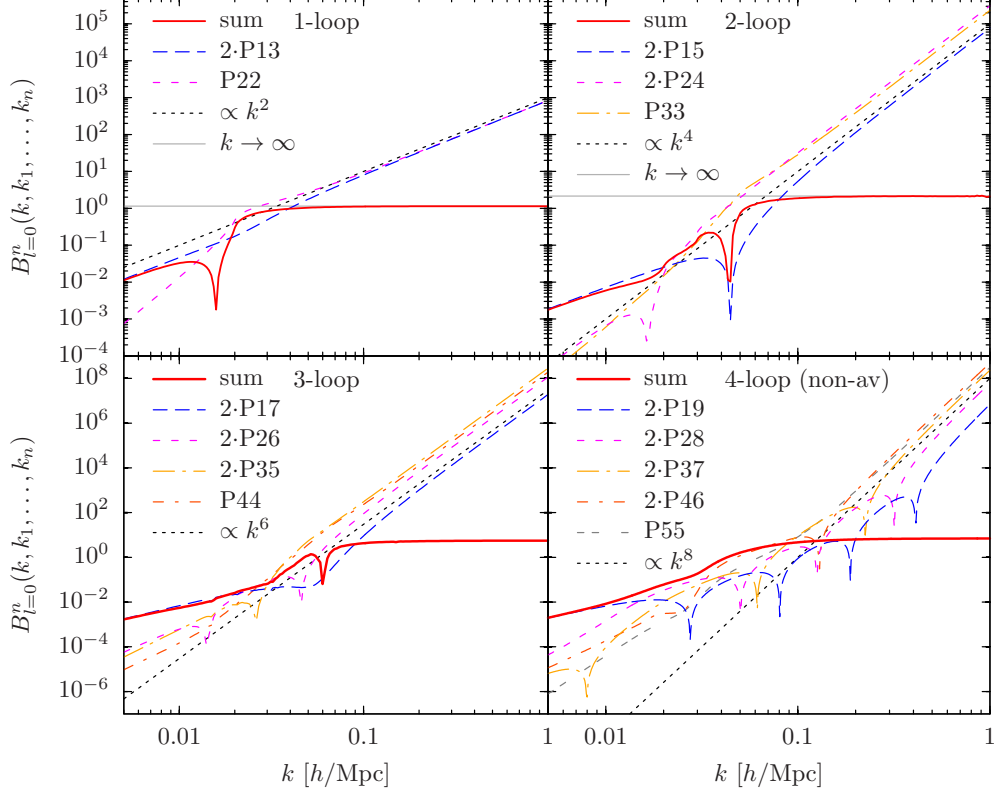


Figure 8: Cancellation of n -loop contributions to the integrand kernels $B_l^{(n)}$ of the power spectrum for $l = 0$. Shown are individual contributions P_{IJ} (dashed lines) which grow like k^{2n} (indicated by the black dotted lines). Their sum yields the kernels $B_l^{(n)}$ (red solid line), which approach a constant value as predicted in Eq. (52). For comparison, the grey lines show the analytical results (65), (71) for the asymptotic value at one and two-loop. For the plot we have chosen $k_1 = 0.02, k_2 = 0.03, k_3 = 0.015, k_4 = 0.019$. For one-, two- and three-loop the kernels are averaged over the angles, see (78). The four-loop case corresponds to (79).

We do not have much to add to this discussion but we want to identify the expansion parameter in this regime and compare it to the large k limit. For

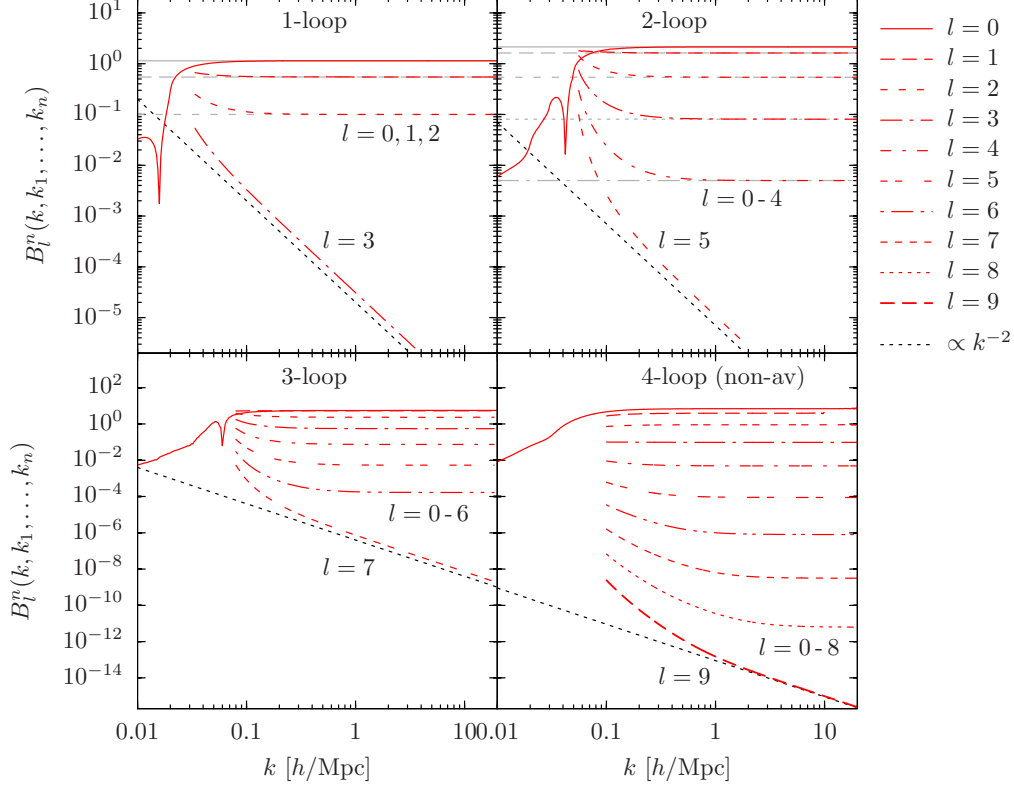


Figure 9: Asymptotic behavior of n -loop integrand kernels B_l^n of the power spectrum for $0 \leq l \leq 2n + 1$ (here only the sum of all individual contributions to each kernel is shown). The kernels with $l \leq 2n$ approach a constant value for large k as predicted in Eq. (52), and go to zero like $\mathcal{O}(k_i^2/k^2)$ for $l > 2n$. Parameters are chosen as in Fig. 8. The grey lines show the analytical large- k results (65), (71) for comparison. For $l > 0$ we show only the range where none of the Heaviside functions contained in the integrand (76) is zero.

the one- and two-loop expressions¹¹, we find

$$\begin{aligned}
 P_{1-loop}(k) &\rightarrow -\frac{61}{105}k^2P^L(k)\frac{4\pi}{3}\int_0^\infty dqP^L(q) = -\frac{61}{105}k^2\sigma_d^2P^L(k), \\
 P_{2-loop}(k) &\rightarrow -\frac{44764}{143325}k^2P^L(k)\frac{4\pi}{3}\int_0^\infty dqP^L(q)J(q), \tag{54}
 \end{aligned}$$

¹¹In the analytic calculations we assume a flat matter-dominated cosmology and only consider the growing mode.

where we introduced the (dimensionless) function

$$J(q) = 4\pi \int_0^q dp p^2 g(p/q) P^L(p). \quad (55)$$

An explicit form for $g(x)$ is given in Appendix B (see also [31]). The relevant aspects are that it is a smooth function satisfying $p^2 g(p/q) = q^2 g(q/p)$. This means that g is almost constant as long as p and q are not of the same order and tends to zero for large argument. Thus, it further cuts-off the integrals of the form (55) at large value of the integration variable. We find $g(0) = 1.54$, $g(1) = 1$ and $g(\infty) \rightarrow 0$. A good approximation for $J(q)$ in the regime of integration of (55) is thus given by taking $g(p/q) \sim 1$, which means that $J(q) \simeq \sigma_l^2(q)$. Therefore, the relative importance of the two-loop results with respect to the one-loop case is again related to the scale $\sigma_l(q)$. Notice, however, that in the low- k case this function is integrated over (cf. (55)).

The previous calculations confirming the results of section 5 can be extended to higher loops. Even if the analytical calculations are very cumbersome in this case, one can still find general arguments about the different behaviors that may be checked with numerical computations. For the large k regime, as long as k is larger than the momenta one integrates over in (51), the results of section 5 imply a roughly constant $B_l^{(n)}$ in (51). If one of the momenta k_i becomes larger than k , additional polynomial suppression $\propto k^2/k_i^2$ arises in the functions $B_l^{(n)}$ what renders the integrals in internal momenta finite. Therefore, k effectively acts as a UV cutoff for the k_i integrations, and one can estimate the integral to contain at n -loop contributions of order ($l \leq 2n$)

$$P_{n-loop} \ni ([k\partial_k]^l P^L(k)) \sigma_l^{2n}(k) \quad (\text{large } k \text{ limit}). \quad (56)$$

Subleading logarithms depend on how the integrals are precisely cut off and can give sizable corrections.

Concerning the low k case, from the symmetries of the integrand in (80) and its behavior at large momenta, one expects the power spectrum to behave as

$$P_{n-loop}(k) \propto k^2 P^L(k) \int_0^\infty dq P^L(q) \sigma_l^{2n-2}(q) \quad (\text{small } k \text{ limit}). \quad (57)$$

As in the previous case, the important expansion parameter for perturbation theory is related to the quantity σ_l^2 .

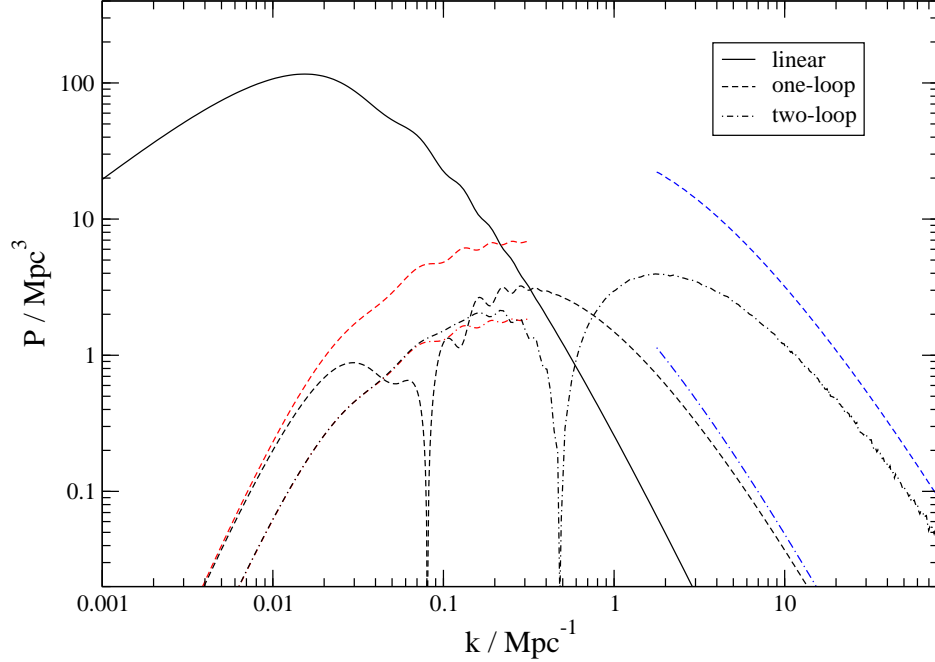


Figure 10: Linear power spectrum and the one- and two-loop corrections in standard perturbation theory at $z = 0$. The linear spectrum corresponds to a Λ CDM cosmology with WMAP5 parameters [29]. The blue lines show the asymptotic behavior at large k (see Eq. (53)), and the red the one at small k (see Eq. (54)).

We have checked the previous asymptotic behavior by computing the power spectrum numerically up to two loops in an Einstein-de Sitter cosmology (taking into account only the growing mode). The results are displayed in Fig. 10. We cross-checked our numerical results for the power spectrum with the RegPT code [29] for momenta where the latter is available. As can be seen in Fig. 10, the asymptotic expressions (54) and (53) agree with the full one- and two-loop results rather accurately. The constant offset in the two-loop case at very large k is expected because (53) captures only the leading logarithmic behavior. It is remarkable that even for very small momenta, the two-loop contribution is only mildly suppressed compared to the one-loop contribution. Naively, one might expect a suppression by a power $k_0^2 \sigma_d^2 \sim \mathcal{O}(10^{-2})$, where k_0 is the position of the maximum of $P^L(k)$. However, the integral over $J(q) \sim \sigma_l^2(q)$ in (54) is sensitive to the power spectrum

at smaller scales, and yields only a mild suppression with respect to the one-loop correction. According to (57), the three-loop result should even exceed the one-loop contribution at asymptotically small momenta for $z = 0$. Actually, we checked numerically for a few values of the momentum that this is indeed the case, and it is also in accordance with the findings of [31]. The same is true for the large k regime. Here, the logarithmic dependence in $\sigma_l^2(k)$ is clearly seen in the numerical results.

7 Discussion

Cosmological perturbation theory provides a very successful framework to understand the gravitational clustering in the Universe, responsible for its structure at the largest scales. Despite of this success, its range of validity (in the sense of convergence of the perturbative series to the non-linear solution) is limited due to the growth of the importance of the non-linear contributions with time. To devise methods that deal with these non-linear corrections it is crucial to understand which effects are behind the failure of perturbation theory. This is even more important when one realizes that a large amount of information about cosmological evolution lies at scales close to the linear scales where these methods may be very useful. An example is provided by the baryonic acoustic oscillations (BAO) at low redshift [3, 32, 33].

A first look at the structure of the standard formulation of cosmological perturbation theory (SPT) singles out the functions

$$k^2 \sigma_d^2(\Lambda, \eta) \equiv \frac{4\pi k^2}{3} \int^\Lambda dq P^L(q, \eta), \quad \sigma_l^2(\Lambda, \eta) \equiv 4\pi \int^\Lambda dq q^2 P^L(q, \eta), \quad (58)$$

as responsible for the failure of the linearized approach for scale k , once one of them becomes big. The first quantity, which is strongly k dependent, is small at the peak of the power spectrum k_0 , $\sigma_d^2 k_0^2 \simeq 0.0135$ at $z = 0$ and $k_0 \simeq 0.02 \text{ Mpc}^{-1}$ (see (47)). This number grows very fast with momenta, which is a consequence of the enhancement coming from the vertex γ_{ijk} for a large hierarchy between the momenta of the two incoming modes, see (7). At n -loop order, this can potentially lead to corrections to the power spectrum that scale at large k as $\propto (k^2 \sigma_d^2)^n P^L(k, \eta)$. It is well known that these leading soft corrections cancel when summing over all n -loop diagrams [11]. However, there are also subleading soft corrections, growing like k^2 at two-loop, like k^4 and k^2 at three-loop, etc. In our analysis we showed that,

when summing over all n -loop diagrams all polynomially growing corrections $\propto k^{2m}$ with $1 \leq m \leq n$ cancel in the limit of large k . This cancellation had not been proven before to the best of our knowledge. Remarkably, the same cancellation happens for any hard skeleton corresponding to n -point correlation functions evaluated at equal-time. While the general proof relies on the eikonal approximation, we also checked explicitly that the subleading k^2 -terms cancel at two-loop, and furthermore checked numerically that all subleading k^{2m} -terms cancel up to four loop order. The cancellation of the leading soft corrections was related to Galilean invariance in [12]. Physically, it seems plausible that similar arguments could explain our results (see e.g. [24, 25]), though we are not aware of any explicit calculation that includes all subleading effects.

Our result also implies that in numerical calculations in SPT it is advantageous to sum over all relevant diagrams (and to symmetrize them appropriately, see the comments after Eq. (79)) before any integration is performed. In this way, the cancellation of different contributions occurs already on the level of the integrand and does not rely on the numerical accuracy of the integration.

Even though the polynomially growing terms cancel, there remains a logarithmic enhancement at large k for the matter power spectrum, see Eq. (51). We find that the leading logarithmic (LL) contributions at large k are given by ¹²

$$P_{n-loop}^{LL}(k, \eta) \simeq \sum_{l=0}^{2n} c_l^{(n)} [k \partial_k]^l P^L(k, \eta) \sigma_l^{2n}(k, \eta), \quad (59)$$

with some coefficients $c_l^{(n)}$ of order unity. This expression implies a growth with k of the expansion parameter $\sigma_l^2(k, \eta)$ which is logarithmic. Note that $\sigma_l^2(k, \eta)$ also controls the loop expansion at the opposite limit of small k , see Eq. (57).

The function $\sigma_l^2(k, \eta)$ is not only sensitive to the high-momentum tail of the spectrum (which makes it increase logarithmically) but for the realistic case (47) it is also numerically rather large for small redshift $z \sim 0$,

$$\sigma_l^2(k, \eta) \simeq 0.15 \left(\frac{1}{1+z} \right)^2 (\ln(e + 1.84\beta k))^3. \quad (60)$$

¹² See Eq. (53) for the explicit expressions at one and two loops.

We find that this function is the true expansion parameter of standard perturbation theory for the equal-time power spectrum. For $k \sim 1 \text{ Mpc}^{-1}$ it is $\sigma_l^2(k, z=0) \sim 3.42$. This large value arises partially due to the logarithmic dependence but also because the initial power spectrum (47) is parametrically enhanced by a factor $(C\beta^2 k_0^2)^{-2} \sim 16$. According to our arguments a smaller value for σ_l would improve the convergence of linearized perturbation theory remarkably. We show this in Appendix C by using a fake initial power spectrum with the same σ_d as ΛCDM but smaller σ_l . The results are shown in Fig. 11, which should be compared with Fig. 10.

Our conclusions about the matter power spectrum also hold for any correlation function at equal times. In these observables, the effects related to the scale σ_d are absent, and the departure from the linear regime will be dominated by σ_l . The analysis is equally valid for arbitrary cosmologies, or even for departures from the standard equations, as the Zel'dovich approximation. We would like to emphasize that this is not the case for other cosmological observables. For instance, the propagator as defined in (21) is certainly affected by the enhancement of soft modes related to the scale σ_d . Its measurement in simulations confirms this behavior [4], and it would be very interesting to extract it from real data. Furthermore, correlations between different redshift bins are also used for lensing tomography [34].

All resummation schemes in the literature resum only certain subsets of diagrams of SPT. Notice that those subsets do not necessarily reproduce the cancellation we found for equal-time correlations. Thus, the non-linearity associated with the scale σ_d may be reintroduced as a purely spurious effect. We would like to emphasize that our results do not imply that standard perturbation theory is superior to resummation schemes as e.g. RPT. It might well be that at intermediate scales, these schemes resum just the right sub-diagrams to lead to accurate results [35]. In addition, they are very useful to describe correlations at unequal times. Still, our analysis supports that at large momenta resummation schemes that involve only the scale σ_d cannot improve the determination of the equal-time correlators systematically. We hope that our results are helpful to identify approximation schemes that respect the cancellation of soft corrections and, at least partially, resum corrections related to the scale σ_l .

Acknowledgements

We would like to thank Martin Kunz, Julien Lesgourgues, Valeria Pettorino, Antonio Riotto and Román Scoccimarro for very useful discussions. DB would like to thank IPMU and DESY for their warm hospitality during the development of this work. This work has been partially supported by the German Science Foundation (DFG) within the Collaborative Research Center 676 “Particles, Strings and the Early Universe”.

A The power spectrum in the hard regime

In this appendix¹³ we discuss the asymptotic behavior of loop corrections to the power spectrum at large wavenumbers k (small scales). It is possible to rewrite the loop contributions such that the cancellation of polynomially growing corrections $\propto k^n P^L(k)$, with $n > 0$, is manifest. We first demonstrate this for the one-loop corrections $P_{1-loop} = 2P_{13} + P_{22}$, with

$$\begin{aligned} P_{13}(k) &= 3P^L(k) \int_q F_3^s(\vec{k}, \vec{q}, -\vec{q}) P^L(q), \\ P_{22}(k) &= 2 \int_q \left[F_2^s(\vec{q}, \vec{k} - \vec{q}) \right]^2 P^L(q) P^L(|\vec{k} - \vec{q}|), \end{aligned} \tag{61}$$

where $F_n^s(\vec{q}_1, \dots, \vec{q}_n)$ are the symmetrized PT kernels entering at the different orders of SPT (see e.g. [2]), $\int_q \equiv \int d^3q$ and $q \equiv |\vec{q}|$. For large k the two contributions asymptotically grow as $P_{13} \rightarrow -k^2 \sigma_d^2 P^L(k)/2$ and $P_{22} \rightarrow k^2 \sigma^2 / 2 P^L(k)$, and it is evident that the quadratically growing corrections cancel [36]. At two-loop, $P_{2-loop} = 2P_{15} + 2P_{24} + P_{33}$, the individual

¹³To improve readability we will not write explicitly the dependence on η in the appendices, since it is trivial to retrieve. In addition we display arrows on three vectors to facilitate discrimination from absolute values.

contributions

$$\begin{aligned}
P_{15}(k) &= 15P^L(k) \int_{p,q} F_5^s(\vec{k}, \vec{p}, -\vec{p}, \vec{q}, -\vec{q}) P^L(p) P^L(q), \\
P_{24}(k) &= 12 \int_{p,q} F_2^s(\vec{q}, \vec{k} - \vec{q}) F_4^s(\vec{q}, \vec{k} - \vec{q}, \vec{p}, -\vec{p}) P^L(p) P^L(q) P^L(|\vec{k} - \vec{q}|), \\
P_{33}(k) &= 9 \int_{p,q} F_3^s(\vec{k}, \vec{p}, -\vec{p}) F_3^s(\vec{k}, \vec{q}, -\vec{q}) P^L(p) P^L(q) \\
&\quad + 6 \int_{p,q} F_3^s(\vec{p}, \vec{q}, \vec{k} - \vec{p} - \vec{q})^2 P^L(p) P^L(q) P^L(|\vec{k} - \vec{p} - \vec{q}|),
\end{aligned} \tag{62}$$

grow asymptotically as $k^4 \sigma_d^4 P^L(k)$. Again, it is straightforward to check that the k^4 terms cancel each other. However, there exist also subleading terms that grow as k^2 . In order to show that they also cancel in the sum of all two-loop contributions, it is convenient to rearrange the various terms. To demonstrate this, we first discuss an analogous rearrangement for the one-loop terms,

$$P_{1L}(k) = P^L(k) \int_q B_0^{(1)}(k, q) P^L(q) + \tilde{P}_{22}(k), \tag{63}$$

where $(d\Omega_q \equiv \sin \theta_q d\theta_q d\phi_q)$

$$\begin{aligned}
B_0^{(1)}(k, q) &\equiv \frac{1}{4\pi} \int d\Omega_q \left(6F_3^s(\vec{k}, \vec{q}, -\vec{q}) + 4F_2^s(\vec{q}, \vec{k} - \vec{q})^2 \right), \\
\tilde{P}_{22}(k) &\equiv 4 \int_q F_2^s(\vec{q}, \vec{k} - \vec{q})^2 P^L(q) \left(\Theta(|\vec{k} - \vec{q}| - q) P^L(|\vec{k} - \vec{q}|) - P^L(k) \right).
\end{aligned} \tag{64}$$

In the latter contribution we subtracted a term $\propto P^L(k)$, such that the difference in the bracket scales as $(\frac{\vec{k}\vec{q}}{k^2} + \mathcal{O}(q^2/k^2))k\partial_k P^L(k)$ for large k . The linear term $\propto \vec{q}/k$ vanishes when integrating, such that the bracket leads to a q^2/k^2 suppression that compensates the quadratic enhancement coming from the kernel $(F_2^s)^2 \sim (\vec{k}\vec{q}/q^2)^2/4$. Note that we also inserted a Heaviside function compared to P_{22} and multiplied by two, which does not change P_{22} due to the symmetry $\vec{q} \rightarrow \vec{k} - \vec{q}$. Using the explicit expressions for the kernels, it is also easy to check that quadratically growing terms $\sim k^2/q^2$ cancel in the combination $B_0^{(1)}$ after averaging over angles (or alternatively symmetrizing

the integrand w.r.t. $\vec{q} \leftrightarrow -\vec{q}$). The explicit result can be easily calculated,

$$\begin{aligned}
B_0^{(1)}(k, q) &= \frac{625}{882} - \frac{11k^4}{294q^4} - \frac{523k^2}{1764q^2} - \frac{q^2}{12k^2} \\
&\quad - \frac{k^2 - q^2}{q^2} \left(\frac{11k^3}{1176q^3} + \frac{9k}{112q} + \frac{8q}{49k} - \frac{q^3}{48k^3} \right) \ln \left(\frac{k - q}{k + q} \right)^2 \\
&\rightarrow \frac{2519}{2205} + \mathcal{O}(q^2/k^2) \quad \text{for } k \rightarrow \infty.
\end{aligned} \tag{65}$$

A similar rearrangement can be done for the two-loop contributions to the power spectrum. In order to extract subleading k^2 -terms apart from the leading k^4 , we have to re-shuffle terms proportional to the first and second derivatives of the power spectrum ($' \equiv d/d \ln k$),

$$P^L(|\vec{k} - \vec{q}|) = P^L(k) + b_1(\vec{k}, \vec{q})P^{L'}(k) + b_2(\vec{k}, \vec{q})P^{L''}(k) + \dots, \tag{66}$$

where

$$b_l(\vec{k}, \vec{q}) = \frac{1}{l!} \left[\ln \left(\frac{|\vec{k} - \vec{q}|}{|\vec{k}|} \right) \right]^l. \tag{67}$$

After this rearrangement, the two-loop contribution can be rewritten as

$$\begin{aligned}
P_{2L}(k) &= P^L(k) \int_{p,q} B_0^{(2)}(k, p, q) P^L(q) P^L(p) \\
&\quad + P^{L'}(k) \int_{p,q} B_1^{(2)}(k, p, q) P^L(q) P^L(p) \\
&\quad + P^{L''}(k) \int_{p,q} B_2^{(2)}(k, p, q) P^L(q) P^L(p) + 2\tilde{P}_{24}(k) \\
&\quad + \tilde{P}_{33}(k),
\end{aligned} \tag{68}$$

where

$$\begin{aligned}
B_l^{(2)}(k, p, q) &\equiv \frac{1}{(4\pi)^2} \int d\Omega_q \int d\Omega_p \left(30F_5^s(\vec{k}, \vec{p}, -\vec{p}, \vec{q}, -\vec{q})\delta_{l0} \right. \\
&\quad + 9F_3^s(\vec{k}, \vec{p}, -\vec{p})F_3^s(\vec{k}, \vec{q}, -\vec{q})\delta_{l0} \\
&\quad + 18F_3^s(\vec{p}, \vec{q}, \vec{k} - \vec{p} - \vec{q})^2 b_l(\vec{k}, \vec{p} + \vec{q}) \\
&\quad + 24F_2^s(\vec{q}, \vec{k} - \vec{q})F_4^s(\vec{q}, \vec{k} - \vec{q}, \vec{p}, -\vec{p})b_l(\vec{k}, \vec{q}) \\
&\quad \left. + 24F_2^s(\vec{p}, \vec{k} - \vec{p})F_4^s(\vec{p}, \vec{k} - \vec{p}, \vec{q}, -\vec{q})b_l(\vec{k}, \vec{p}) \right),
\end{aligned} \tag{69}$$

for $l = 0, 1, 2$ with $b_0 \equiv 1$, and

$$\begin{aligned}
\tilde{P}_{24}(k) &\equiv 24 \int_{p,q} F_2^s(\vec{q}, \vec{k} - \vec{q}) F_4^s(\vec{q}, \vec{k} - \vec{q}, \vec{p}, -\vec{p}) P^L(p) P^L(q) \left(\Theta(|\vec{k} - \vec{q}| - q) \right. \\
&\quad \times P^L(|\vec{k} - \vec{q}|) - P^L(k) - b_1(\vec{k}, \vec{q}) P^{L'}(k) - b_2(\vec{k}, \vec{q}) P^{L''}(k) \Big), \\
\tilde{P}_{33}(k) &\equiv 18 \int_{p,q} F_3^s(\vec{p}, \vec{q}, \vec{k} - \vec{p} - \vec{q})^2 P^L(p) P^L(q) \left(\Theta(|\vec{k} - \vec{p} - \vec{q}| - q) \right. \\
&\quad \times \Theta(|\vec{k} - \vec{p} - \vec{q}| - p) P^L(|\vec{k} - \vec{p} - \vec{q}|) - P^L(k) - b_1(\vec{k}, \vec{p} + \vec{q}) P^{L'}(k) \\
&\quad \left. - b_2(\vec{k}, \vec{p} + \vec{q}) P^{L''}(k) \right). \tag{70}
\end{aligned}$$

The subtracted terms inside the brackets in the last two expressions are constructed such that, after angular integration, they compensate the terms growing as k^4 and k^2 coming from the PT kernels for $k \rightarrow \infty$. Thus, it remains to be shown that the functions $B_l^{(2)}$ in (68) do not grow with k . For that purpose, we expand the integrand for large k and use that the angular integration can equivalently be performed over k and p while keeping the direction of q fixed along the z -axis (see e.g. [12]). We find that indeed the k^4 and k^2 terms cancel. For the leading contributions in the limit $k \rightarrow \infty$ (which are $\propto k^0$) we find

$$\begin{aligned}
B_0^{(2)}(k, p, q) &\rightarrow \frac{271133}{92702610} \left(f(p/q) + \frac{595172936}{813399} \right) + \mathcal{O}(1/k^2), \\
B_1^{(2)}(k, p, q) &\rightarrow \frac{5377}{12677280} \left(f(p/q) - \frac{308888266}{80655} \right) + \mathcal{O}(1/k^2), \\
B_2^{(2)}(k, p, q) &\rightarrow \frac{115}{32928} \left(-f(p/q) + \frac{452758}{2875} \right) + \mathcal{O}(1/k^2), \\
B_3^{(2)}(k, p, q) &\rightarrow \frac{3}{3920} \left(f(p/q) - \frac{4882}{45} \right) + \mathcal{O}(1/k^2), \\
B_4^{(2)}(k, p, q) &\rightarrow \frac{1}{200} + \mathcal{O}(1/k^2), \tag{71}
\end{aligned}$$

where

$$f(x) \equiv \frac{8x^2}{3} + \frac{8}{3x^2} - x^4 - \frac{1}{x^4} - \frac{1}{4x^5} (x^2 + 1)(x^2 - 1)^4 \ln \left(\frac{x-1}{x+1} \right)^2. \tag{72}$$

The results for $l = 3, 4$ are shown for later use, and $B_l^{(2)} = \mathcal{O}(1/k^2)$ for $l \geq 5$. For completeness, we also quote the large- k limits for the higher-derivative

contributions at one-loop which are given by

$$B_1^{(1)}(k, q) \rightarrow -\frac{23}{42}, \quad B_2^{(1)}(k, q) \rightarrow \frac{1}{10}, \quad B_{l \geq 3}^{(1)}(k, q) \rightarrow \mathcal{O}(1/k^2). \quad (73)$$

The rearrangement presented above is useful to show that polynomially growing corrections cancel out. The leading correction for large k is thus a logarithmic one. It is possible to extract an analytic expression for the leading logarithmic corrections by performing a similar rearrangement, but including terms up to $[k\partial_k]^2 P^L$ at one-loop and up to the fourth derivative $[k\partial_k]^4 P^L$ at two-loop. This yields approximate expressions for large k

$$\begin{aligned} P_{1-loop}(k) &\rightarrow \left(\frac{2519}{2205} P^L(k) - \frac{23}{42} k \partial_k P^L(k) + \frac{1}{10} [k\partial_k]^2 P^L(k) \right) \sigma_l^2(k), \quad (74) \\ P_{2-loop}(k) &\rightarrow (4\pi)^2 \sum_{l=0}^4 [k\partial_k]^l P^L(k) \int_0^k dq q^2 P^L(q) \int_0^k dp p^2 P^L(p) B_l^{(2)}(k, p, q) \\ &\sim \left(\frac{1490372537}{695269575} P^L(k) - \frac{7719787}{4753980} k \partial_k P^L(k) + \frac{112327}{205800} [k\partial_k]^2 P^L(k) \right. \\ &\quad \left. - \frac{1207}{14700} [k\partial_k]^3 P^L(k) + \frac{1}{200} [k\partial_k]^4 P^L(k) \right) \sigma_l^4(k). \quad (75) \end{aligned}$$

Here we assumed that the main contribution to the integrals in (75) comes from the integration range $p, q < k$, which given the form (47) is valid at high k up to logarithmic corrections. Besides, in the last line we substituted $f(p/q) \sim 1$, which is valid for $p \ll q$ (or, equivalently, $q \ll p$). One can easily get convinced that this estimate is adequate for $f(x)$ given by (72).

It is straightforward to extend the rearrangement to n loops. The n -loop contribution given in Eq. (49) can be rewritten by integrating over k_1 . Due to the symmetry in the momenta k_1, \dots, k_m , one may restrict the range of integration to the case where $|k_1|$ is larger than any of the $|k_i|$ for $1 < i \leq m$, and multiply by a factor m ,

$$\begin{aligned} P_{n-loop}(k, \eta) &= \sum_{m=1}^{n+1} m \int d^3 k_2 \dots d^3 k_{n+1} A_m^{(n)}(\vec{k}_1, \dots, \vec{k}_{n+1}) \\ &\quad \times \Theta(|k_1| - |k_2|) \times \dots \times \Theta(|k_1| - |k_m|) \\ &\quad \times P^L(k_1, \eta) \dots P^L(k_{n+1}, \eta) \Big|_{\vec{k}_1 = \vec{k} - \vec{k}_2 \dots - \vec{k}_m}. \quad (76) \end{aligned}$$

The integration kernels in the notation of Eq. (49) are given by

$$\begin{aligned}
A_m^{(n)}(\vec{k}_1, \dots, \vec{k}_{n+1}) &= \sum_{n_L=0}^{n-m+1} \frac{(2n_L+m)!(2n_R+m)!}{2^{n_L+n_R} m! n_L! n_R!} \\
&\times F_{2n_L+m}^s(\vec{k}_1, \dots, \vec{k}_m, \vec{p}_1, -\vec{p}_1, \dots, \vec{p}_{n_L}, -\vec{p}_{n_L}) \\
&\times F_{2n_R+m}^s(\vec{k}_1, \dots, \vec{k}_m, \vec{q}_1, -\vec{q}_1, \dots, \vec{q}_{n_R}, -\vec{q}_{n_R}), \quad (77)
\end{aligned}$$

where $n_R \equiv n+1-m-n_L$, $\vec{p}_i \equiv \vec{k}_{m+i}$, $\vec{q}_i \equiv \vec{k}_{m+n_L+i}$. In the usual P_{IJ} notation, a given term in the sum in (77) contributes to $P_{2n_L+m, 2n_R+m}$. Diagrammatically, a given summand corresponds to a diagram with two ‘blobs’ that are connected by m lines, and have n_L and n_R lines connected to themselves. By adding and subtracting the terms obtained from a Taylor expansion of $P^L(k_1, \eta_0)$ around k up to order $2n$, one obtains the rearrangement analogous to the one- and two-loop case discussed above. The coefficients of the terms containing the Taylor-expanded power spectrum in (51) after the rearrangement are

$$B_l^{(n)}(k, k_1, \dots, k_n) \equiv \frac{1}{(4\pi)^n} \int d\Omega_{k_1} \cdots \int d\Omega_{k_n} B_l^{(n)}(\vec{k}, \vec{k}_1, \dots, \vec{k}_n), \quad (78)$$

where

$$\begin{aligned}
B_l^{(n)}(\vec{k}, \vec{k}_1, \dots, \vec{k}_n) &= A_1^{(n)}(\vec{k}, \vec{k}_1, \dots, \vec{k}_n) \delta_{l0} \\
&+ \sum_{m=2}^{n+1} m A_m^{(n)}(\vec{k} - \vec{k}_1 \cdots - \vec{k}_{m-1}, \vec{k}_1, \dots, \vec{k}_n) \\
&\times b_l(\vec{k}, \vec{k}_1 + \cdots + \vec{k}_{m-1}) \Big|_{\text{symm}}. \quad (79)
\end{aligned}$$

Here, the right-hand side is to be fully symmetrized w.r.t. permuting the \vec{k}_i and w.r.t. inverting the sign $\vec{k}_i \rightarrow -\vec{k}_i$ of each momentum. We note that in our numerical results (up to four loop order) we find that the cancellation of terms growing with k can even be observed at the level of the non-averaged expression.

B The power spectrum in the soft regime

In the limit $k \rightarrow 0$, the dominant contribution to the n -loop correction to the power spectrum is given by [27, 37]

$$P_{n-loop}(k) \rightarrow 2(2n+1)!! P^L(k) \int_{q_1} \cdots \int_{q_n} F_{2n+1}^s(\vec{k}, \vec{q}_1, -\vec{q}_1, \dots, \vec{q}_n, -\vec{q}_n) \times P^L(q_1) \cdots P^L(q_n). \quad (80)$$

Due to the well-known property $F_{2n+1}^s \propto k^2$ of the PT kernels [30], these corrections scale as $k^2 P^L(k)$. All other loop corrections would lead to terms scaling as k^4 or $k^4 P^L(k)$, respectively, that are parametrically smaller for $k \rightarrow 0$ for a power spectrum $P^L(k) \propto k^{n_s}$ with $n_s \lesssim 1$. The function appearing in the two-loop correction (54) is given by

$$g(x) = \frac{1}{179056x^6} \left((x^2 + 1)(128258x^4 - 5760(x^8 + 1) - 13605(x^6 + x^2)) - \frac{15}{4x}(x^2 - 1)^4(384(x^4 + 1) + 2699x^2) \ln \left(\frac{x-1}{x+1} \right)^2 \right). \quad (81)$$

C Convergence and fictitious power spectra

In this section, we present a two-loop result for a fictitious power spectrum with better convergence behavior than (47). Let us consider an initial power spectrum of the form

$$P_0(k) \propto \frac{k k_0}{k_0^5 + k^5}. \quad (82)$$

This spectrum is chosen such that the expansion parameter of standard perturbation theory σ_l^2 is not sensitive to the high momentum part of the spectrum. Hence σ_l^2 is small as long as $k_0^2 \sigma_d^2$ is much smaller than unity. Fig. 11 shows a power spectrum with $k_0^2 \sigma_d^2 \simeq 0.015$ and $\sigma_l^2 \simeq 0.02$. Even though $k_0^2 \sigma_d^2$ is as large as in the physical case at $z \sim 0$, the two-loop result is well below the one-loop contribution and standard perturbation theory is expected to converge. Compare with Fig. 10.

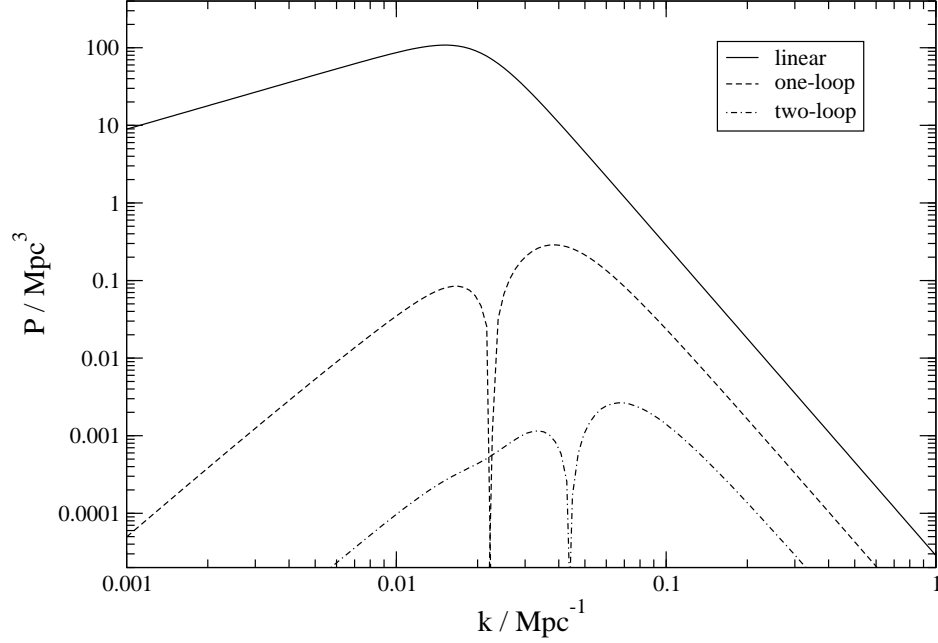


Figure 11: Example for a power spectrum where σ_l^2 is not sensitive to the high momentum region. The different lines are the linear, one-loop and two-loop contributions. The corresponding parameters are $k_0^2 \sigma_d^2 \simeq 0.015$ and $\sigma_l^2 \simeq 0.02$.

References

- [1] P. J. E. Peebles, “The Large-Scale Structure of the Universe” (Princeton University Press, 1980)
- [2] F. Bernardeau, S. Colombi, E. Gaztanaga and R. Scoccimarro, Phys. Rept. **367** (2002) 1 [astro-ph/0112551].
- [3] M. Crocce and R. Scoccimarro, Phys. Rev. D **73** (2006) 063519 [astro-ph/0509418].
- [4] M. Crocce and R. Scoccimarro, Phys. Rev. D **73** (2006) 063520 [astro-ph/0509419].
- [5] A. Taruya and T. Hiramatsu, Astrophys. J. **674**, (2008) 617 , arXiv:0708.1367 [astro-ph].

- [6] S. Matarrese, M. Pietroni and , JCAP **0706** (2007) 026 [astro-ph/0703563].
- [7] P. Valageas, A & A, **465** (2007) 725-747, [arXiv:astro-ph/0611849]
- [8] T. Matsubara, Phys. Rev. D **77** (2008) 063530 [arXiv:0711.2521 [astro-ph]].
- [9] M. Pietroni, JCAP **0810** (2008) 036 [arXiv:0806.0971 [astro-ph]].
- [10] S. Anselmi and M. Pietroni, JCAP **1212** (2012) 013 [arXiv:1205.2235 [astro-ph.CO]].
- [11] B. Jain and E. Bertschinger, Astrophys. J. **456** (1996) 43 [astro-ph/9503025].
- [12] R. Scoccimarro and J. Frieman, Astrophys. J. Suppl. **105** (1996) 37 [astro-ph/9509047].
- [13] F. Bernardeau, N. Van de Rijt and F. Vernizzi, Phys. Rev. D **85** (2012) 063509 [arXiv:1109.3400 [astro-ph.CO]].
- [14] F. Bernardeau, N. Van de Rijt and F. Vernizzi, Phys. Rev. D **87** (2013) 043530 [arXiv:1209.3662 [astro-ph.CO]].
- [15] J. J. M. Carrasco, M. P. Hertzberg and L. Senatore, JHEP **1209**, 082 (2012) [arXiv:1206.2926 [astro-ph.CO]].
- [16] M. Pietroni, G. Mangano, N. Saviano, M. Viel and , JCAP **1201** (2012) 019 [arXiv:1108.5203 [astro-ph.CO]].
- [17] R. Scoccimarro, Mon. Not. Roy. Astron. Soc. **299** (1998) 1097 [astro-ph/9711187].
- [18] Y. .B. Zeldovich, Astron. Astrophys. **5** (1970) 84.
- [19] P. Valageas, [arXiv:0706.2593 [astro-ph]].
- [20] L. Hui and E. Bertschinger, Astrophys. J. **471** (1996) 1 [astro-ph/9508114].
- [21] H. W. Wyld, Ann. Phys. **14** 143, (1961).

- [22] V. L’vov and I. Procaccia, chao-dyn/9502010, *Lecture Notes on the Les Houches 1994 Summer School* (1995)
- [23] F. Bernardeau, M. Crocce and R. Scoccimarro, Phys. Rev. D **78** (2008) 103521 [arXiv:0806.2334 [astro-ph]].
- [24] M. Peloso and M. Pietroni, JCAP **1305** (2013) 031 [arXiv:1302.0223 [astro-ph.CO]].
- [25] A. Kehagias and A. Riotto, Nucl. Phys. B **873** (2013) 514 [arXiv:1302.0130 [astro-ph.CO]].
- [26] N. S. Sugiyama and T. Futamase, Astrophys. J. **769** (2013) 106 [arXiv:1303.2748 [astro-ph.CO]].
- [27] J. N. Fry, Astrophys. J. **421** (1994) 21.
- [28] D. J. Eisenstein and W. Hu, Astrophys. J. **511** (1997) 5 [astro-ph/9710252].
- [29] A. Taruya, F. Bernardeau, T. Nishimichi and S. Codis, Phys. Rev. D **86** (2012) 103528 [arXiv:1208.1191 [astro-ph.CO]].
- [30] M. H. Goroff, B. Grinstein, S. J. Rey and M. B. Wise, Astrophys. J. **311** (1986) 6.
- [31] F. Bernardeau, A. Taruya and T. Nishimichi, “Cosmic propagators at two-loop order,” arXiv:1211.1571 [astro-ph.CO].
- [32] D. J. Eisenstein, H. -j. Seo, M. J. White, 1 and , Astrophys. J. **664** (2007) 660 [astro-ph/0604361].
- [33] D. H. Weinberg, M. J. Mortonson, D. J. Eisenstein, C. Hirata, A. G. Riess, E. Rozo and , arXiv:1201.2434 [astro-ph.CO].
- [34] W. Hu, Astrophys. J. **522** (1999) L21 [astro-ph/9904153].
- [35] F. Bernardeau, M. Crocce, R. Scoccimarro and , Phys. Rev. D **85** (2012) 123519 [arXiv:1112.3895 [astro-ph.CO]].
- [36] E. T. Vishniac, Mon. Not. Roy. Astron. Soc. **203** (1983) 345
- [37] P. Valageas, A & A, **382** (2002) 477 - 487, [arXiv:astro-ph/0109408].